Central European Journal of Energetic Materials, **2005**, *2*(2), 29-44.
ISSN 1733-7178

The Elimination of NO_2 from Mixtures of the Nitramines HMX, RDX and CL20 with the Energetic Binder Glycidyl Azide Polymer (GAP) – A Computational Study I

Manfred A. BOHN

Fraunhofer Institut für Chemische Technologie, Energetic Materials Stability, Joseph-von-Fraunhofer-Str. 7, D-76327 Pfinztal (Berghausen), Germany

Anton HAMMERL, Kate HARRIS and Thomas M. KLAPÖTKE*

Department of Chemistry and Biochemistry, Ludwig-Maximilians Universität München (LMU), Butenandtstr. 5-13 (D), D-81377 München, Germany
**E-mail: tmk@cup.uni-muenchen.de*

Abstract: The energetic plasticizer glycidyl azide polymer (GAP) is used for new types of rocket propellants which are formulated with the objective of achieving higher burning rates. The reaction profiles for several possible initial steps in the decomposition of mixtures of the nitramines octahydro-1,3,5,7-tetranitro-1,3,5,7-tetrazacyclooctane (HMX), hexahydro-1,3,5-trinitro-1,3,5-triazine (RDX) and hexanitrohexaazaisowurtzitane (CL20) with a monomer of GAP-diol have been examined computationally. Comparison of the activation energies for the decomposition of the mixtures with those for the decomposition of the isolated nitramines shows that the presence of GAP-diol decreases the activation energy for the elimination of NO_2 by at least to 8 kJ mol^{-1} for CL20, wheras the NO_2 elimination from HMX is only favored by 1 kJ mol^{-1} and NO_2 elimination from RDX is inhibited in the presence of GAP-diol by 2 kJ mol^{-1}.

Keywords: calculation, decomposition, energetic binder, nitramine, solid rocket propellants

Introduction

A mixture of the nitramine CL20 (hexanitrohexaazaisowurtzitane) with the energetic binder GAP is being developed as a base for a new faster burning rocket propellant [1, 2]. Experimental investigation has shown that the decomposition reactions of mixtures of ε-CL20 and β-HMX with GAP proceed in different ways. Mixtures of CL20 with GAP decompose more quickly and with an autocatalytic increase in rate, whereas the decomposition of mixtures of HMX with GAP shows simply a linear increase in reactivity [3].

In this report, the initial step of the gas-phase decomposition of the nitramines HMX, RDX and CL20 with a monomer of GAP-diol is modeled computationally in order to gain a better understanding of the complex processes involved in the decomposition of these mixtures. Here we focus on the elimination of NO_2, which is the initial decomposition step with the lowest activation energy, another paper will deal with other possible initial decomposition steps.

Results and Discussion

The decomposition of the isolated nitramines is discussed first in order to identify similarities and differences in the behavior of the mixtures of the nitramines with GAP-diol.

Decomposition of HMX

The decomposition of HMX has a complex mechanism, since many processes may occur simultaneously. The decomposition depends on the temperature, pressure, heating rate, particle size and purity of the sample. As a result, reported experimental findings can appear contradictory if they are obtained under different experimental conditions. Reported decomposition temperatures range from 230 [4, 5] to 277 °C [6]. Explosive decomposition at 257 °C [7] and melting at 270 °C [8] have also been reported, although the actual melting point is 282 °C. The main products [9-11] of the decomposition are the small, gaseous molecules N_2O, CH_2O, H_2O, CO, NO and HCN. Small amounts of *N*-methylformamide, dimethylnitrosamine, dimethylformamide and octahydro-1-nitroso-3,5,7-trinitro-1,3,5,7-tetrazacylclooctane (ONTNTA) have also been reported. A non-volatile residue with a polyamide structure, comprising 3.5% of the total sample, remaining after the decomposition is complete [10, 11].

The decomposition of HMX is a first order [5] autocatalytic reaction [9-11] with characteristic initiation, acceleratory and decay phases [4, 7, 9, 16]. Each of

these phases corresponds to a different physical state and a different rate-determining step [7] and therefore to the formation of different products [9-11]. Kinetic isotope effects show that the reaction rate of the induction phase, in which HMX is still in the solid state, is determined by C-H bond fission [4, 12]. In the following acceleratory, or mixed-melt phase, the rate of decomposition is determined by the destruction of inter- and intramolecular hydrogen bonds. C-N bond fission is the rate determining step in the decay phase, in which HMX is completely molten. A common rate determining step has also been proposed for the first two phases [4].

In the first phase N_2O, CH_2O and NO [9-11] are observed. In the second, the concentration of these compounds increases and H_2O, CO and the amide products are detected. Water is believed to catalyze further decomposition and to influence the decomposition of the methylene nitramine intermediate [11-13]. ONTNTA, HCN and methylformamide are produced later in the decomposition process [9].

The N-NO_2 bond is the weakest bond in the HMX molecule. Hence, N-NO_2 bond fission has been identified as the most important initial step in the decomposition [5, 11, 13-16]. Several other unimolecular decomposition pathways have been proposed for the decomposition of HMX (Scheme 1, Table 1) [16].

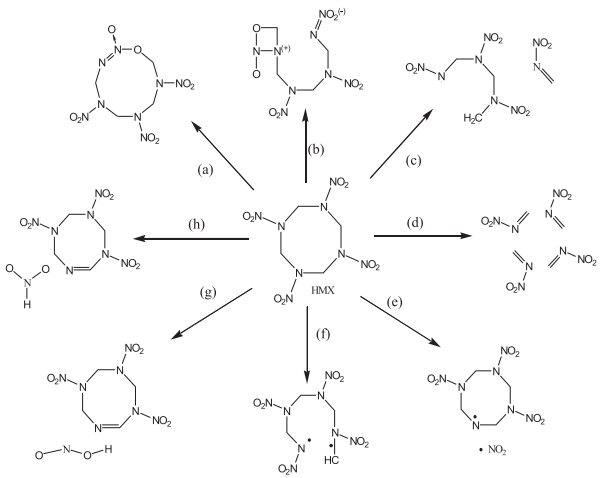

Scheme 1. Proposed pathways for the first step in the decomposition of HMX. (a) Transfer of an oxygen atom from an NO_2 group to an adjacent CH_2 group. (b) Heterolytic C-N bond fission. (c) Elimination of H_2CNNO_2. (d) Concerted depolymerization to four molecules of H_2CNNO_2. (e) Homolytic N-NO_2 bond fission. (f) Homolytic C-N bond fission. (g) Elimination of HONO (nitrous acid). (h) Elimination of HNO_2 (nitrous acid).

Experimentally determined values for the activation energy of the decomposition of HMX lie between 208.4 kJ mol^{-1} [4] and 221.0 kJ mol^{-1} [5]. N-NO_2 bond fission might be accompanied by an intramolecular C-H bond fission because the activation energy of the rate determining C-H bond fission is much higher than any experimentally determined activation energy for the decomposition of HMX. Alternatively, a cage effect has been proposed, which is in accordance with an initial homolysis of N-NO_2, followed by a rate determining C-H bond fission [7, 12]. The radical produced during the N-NO_2 bond fission is believed to decompose to a H_2CN radical and three molecules of both N_2O and CH_2O. This could occur *via* the stepwise elimination of three molecules of CH_2NNO_2 [5, 11-13, 15]. This mechanism is supported by experimental molar product ratios [5, 11] and isotope scrambling experiments which show that the N-N bond in N_2O is not broken [11, 12]. Although N-NO_2 bond fission is the most energetically favorable initial step in the decomposition, the endothermicity associated with further decomposition through ring-opening or subsequent N-NO_2 fissions makes the overall pathway less favorable [15]. The consecutive elimination of four molecules of HONO has been calculated as a lower energy decomposition pathway [15].

Decomposition of RDX

As expected, the decomposition mechanisms of RDX and HMX are very similar, but have some important differences. All products found in the decomposition of HMX are also found in that of RDX. Three further decomposition products have been detected for RDX only: NO_2, [4, 17, 18 -19] HONO, [4, 17, 19] and an oxy-*s*-triazine compound (OST), [4, 17, 19] the exact structure of which is not known. The decomposition of RDX begins slightly below its melting point of 200 °C, [4, 17, 19, 20] which means that the decomposition occurs in the liquid phase. In contrast to HMX, water does not seem to catalyze the decomposition [17, 19]. However, an NO_2 catalyst has been proposed [5].

Although very little decomposition takes place in the solid state, classic induction and acceleratory phases have been found for this stage of the decomposition [17]. The main product of this process is the mononitroso equivalent of RDX, which decomposes further to N_2O and CH_2O. The presence of CH_2O in the crystal lattice initiates the melting of RDX. It is believed that the rate of decomposition is increased due to the change of state of RDX, and not as a result of autocatalytic processes [17]. However, a distinctive induction phase was not found [4].

The time dependence of the appearance of the products leads to the

conclusion that four parallel decomposition pathways occur in the liquid phase. Two unimolecular decomposition pathways, which together account for 40% of the total decomposition, lead to OST, H_2O, NO and NO_2, and NO_2, H_2CN, NO and CH_2O, respectively. A third pathway, accounting for 30% of the decomposition, involves reaction with NO and yields the nitroso equivalent of RDX, which in turn decomposes to N_2O and CH_2O. The fourth process, which requires an as yet unknown catalyst, also accounts for 30% of the decomposition and gives N_2O, CH_2O, NO_2 and formamide. This catalytic path explains the large amounts of some products remaining even after the sample of RDX has almost completely decomposed.

Experimental [5, 18] and theoretical [21, 22] evidence show N-NO_2 bond fission to be the most important initial step in the decomposition of RDX, as found for HMX [5, 11, 13-16]. The other initial processes in the decomposition, shown in Scheme 1, are also valid for RDX. A summary of calculated activation energies is shown in Table 1.

There is both theoretical and experimental evidence to show that the concerted depolymerization reaction to CH_2NNO_2 molecules is more energetically favorable for RDX than for HMX [20]. The calculated activation energies for oxygen atom transfer from an NO_2 group to an adjacent CH_2 group are of the same magnitude as those for concerted depolymerization [22].

Isothermal analysis gave an activation energy of 158.2 kJ mol^{-1} for the decomposition of RDX [5]. Kinetic isotope effects suggest that C-H bond fission is the rate determining step. Again, it is possible that N-NO_2 and C-H bond fission occur simultaneously, as discussed above for HMX. This mechanism is supported by the short intramolecular O···H contacts in the molecule [23].

The successive elimination of three HONO molecules has been calculated as the most energetically favorable decomposition path, although the decomposition of the resulting intermediate is highly endothermic [22]. As for the decomposition of HMX, the highly endothermic processes required after an initial N-NO_2 bond fission make this pathway less favorable overall [22]. However, this mechanism is supported by experimental molar product ratios and the lack of isotope scrambling in the N_2O formed during the decomposition. After oxygen atom transfer from an NO_2 group to an adjacent CH_2 group, the intermediate can decompose in a concerted fashion to form CH_2O, N_2O and methylene nitramine [15].

Decomposition of CL20

The decomposition of CL20 is similar to the decomposition of RDX and HMX and subject to the same parameters, but is an even more complex process.

Most of the differences can be attributed to the lower thermal stability of CL20 as compared to the cyclic nitramines. This is caused by the strained cage structure and higher density of CL20. The more complex substituents on the nitramine groups in CL20 provide more reaction pathways after the initial decomposition step. Consequently, fewer endothermic reactions are possible after the initial decomposition step, and hence the stability of the molecule is reduced [5].

The decomposition of CL20 occurs at around 200 °C [24-27] at a rate two orders of magnitude faster than that of HMX [24]. The process is a first order reaction with second order autocatalysis, [28] although autocatalysis was not observed in all studies [25]. In contrast to the cyclic nitramines, where the decomposition takes place primarily in the liquid phase, the decomposition of CL20 mainly occurs in the solid state [24].

A large amount of solid residue (9-18%) remains after the decomposition of CL20, which produces primarily CO_2, N_2O, NO_2 and HCN [26,27]. Traces of NO, CO, [26, 27] HONO, HNCO [25] and H_2O [26] have also been detected. The ratio of the main products remains constant until maximum concentrations of NO_2 and N_2O are reached. Thereafter, the concentration of N_2O stays constant, that of NO_2 decreases and those of CO_2 and HCN increase [25-27]. The amorphous residue, which contains C=O, C=N and N-H bonds, is believed to be a polyamide or polyazine [24-27, 29]. At temperatures above 700 °C the residue decomposes entirely to give gaseous products, mainly HNCO and HCN [26, 29].

As observed for the other nitramines, the initial step in the decomposition of CL20 is assumed to be a homolytic N-NO_2 bond fission [5, 25-27]. An activation energy of 177 kJ mol^{-1} has been determined for a solution of CL20 in acetone [5]. Kinetically determined activation energies of 185.4 ±4 kJ mol^{-1} [26, 28] and 172 ±26 kJ mol^{-1} [27] have been reported for the non-catalyzed part of the decomposition. These values are slightly lower than the typical N-NO_2 bonding energy due to the strained cage structure of CL20. Low temperature EPR photolysis has shown that there is no preference for the homolysis of a particular nitramine group [30-32].

A recent theoretical study finds that the N-N bond fission reaction during the elimination of NO_2 is the most favorable process for the initial decomposition of CL20 [33].

All nitro groups are lost from CL20 by a temperature of 285 ° [29]. The resulting NO_2 radicals remain trapped in the crystal lattice, [30-32] where they can react with other radicals which form in the cage structure, [25-27] thus accelerating the decomposition [26]. It is possible that the C-N bond strength is

increased by the formation of multiple bonds, [25] which would explain the presence of C=N double bonds in the solid residue. It is also possible that the formation of radical structures in the crystal lattice results in the breakdown of the cage structure and the formation of N_2O, CO_2 and HCN [26, 27].

Computational Results

We have calculated the ground states of the nitramines and GAP-diol at the B3LYP/6-31G(d) level of theory. The β-conformer of HMX was found to be 9.41 kJ mol^{-1} (7.91 kJ mol^{1} with *zpe*) lower in energy than α-HMX, which is in agreement with the literature values of 10.46, [15] 9.75 [14] and 9 kJ mol^{1} [8]. The diaxial conformation of RDX was found to be favored by 0.30 kJ mol^{-1} (0.75 kJ mol^{1} with *zpe*) over the triaxial conformation, by 1.32 kJ mol^{-1} (5.25 kJ mol^{-1} with *zpe*) over the monoaxial conformation and by 5.43 kJ mol^{-1} (20.76 kJ mol^{1} with *zpe*) over the triequatorial conformation. Whilst the triaxial form has been reported as the minimum energy conformation, the diaxial conformation was not considered in the report [22]. Other reports have also found the diaxial conformation to be the global minimum [23]. The relatively small energy differences between the conformers allow a fast conformational exchange in the gas phase, with the triaxial form as the averaged geometry. The β-polymorph of CL20 is 4.74 kJ mol^{-1} (3.92 kJ mol^{1} with *zpe*) lower in energy than γ-CL20 and 6.79 kJ mol^{1} (5.99 kJ mol^{-1} with *zpe*) lower in energy than the ε-polymorph. For all further calculations, we used β-HMX, which is also the most stable polymorph of HMX in the solid phase, diaxial RDX and ε-CL20, which is the most stable solid-state polymorph of CL20.

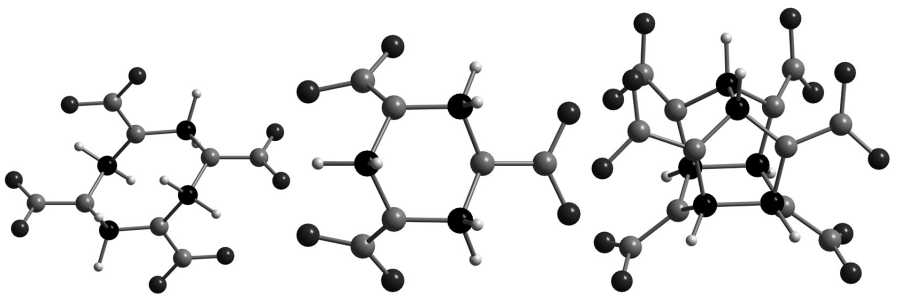

Figure 1. Conformations of the nitramines used in the calculations: β-HMX, diaxial RDX and ε-CL20.

We then determined the transition states for the decomposition pathways given in Scheme 1 at the B3LYP/6-31G(d) level of theory, which has been applied in previous studies [15, 22]. As discussed above, the decomposition pathways given in Scheme 1 for HMX also apply, with some deviations, for RDX and CL20.

Here we focus on the N-NO_2 bond breaking reaction, the other decomposition pathways will be discussed in a later report.

Table 1. Calculated activation energies for the hemolytic N-NO_2 bond fission (path e in Scheme 1).

HMX	Ea kJ mol^{-1}	RDX	Ea kJ mol^{-1}	CL20	Ea kJ mol^{-1}
B3LYP/6-31G(d) (β HMX) [15]	166.5	BPW 91/ /cc-pVDZ [21]	143.5	solution of CL20 in acetone [5]	177
B3LYP/cc-pVDZ (α HMX) [13]	166.2	B3LYP/ /6-31G(d) [22]	163.2	B3LYP/ /6-31G(d) [33]	157.4
Comparison of bond breaking energies [16]	193.3				
BLYP/6-311G(d,p) (β HMX) [14]	174.9				
B3LYP/6-311G(d,p) (α HMX) [14]	169.5				
B3LYP/6-31G(d)[a]	178.5		173.2		-
B3LYP/3-21G[a]	162.8		152.1		153.1
Mixture with GAP at B3LYP/3-21G / I[a]	161.2		174.0		151.7
Mixture with GAP at B3LYP/3-21G / II[a]	169.3		154.7		145.4

[a] this investigation

We repeated the calculations of the transition states at the B3LYP/3-21G level of theory. It was necessary to use this very small basis set as the high computational cost associated with using a larger basis set would have prevented the inclusion of the GAP-diol molecule in the calculations. Table 1 shows that we found lower bond breaking energies with the smaller basis set for all nitramines. The differences for RDX (21.1 kJ mol^{-1}) and for HMX (15.7 kJ mol^{-1}) are quite large, whereas it is only 4.3 kJ mol^{-1} for CL20. We therefore expect the actual activation energies to be higher than the calculated ones.

Thereafter, the transition states of mixtures of the nitramines with a monomer of GAP-diol were calculated. In order to evaluate the effect of different alignments

of GAP-diol on the activation energies, two different alignments were used. Alignment I is the minimum energy arrangement of the respective nitramines with GAP-diol, and alignment II was specifically chosen for the interaction of the azide groups with a nitramine group.

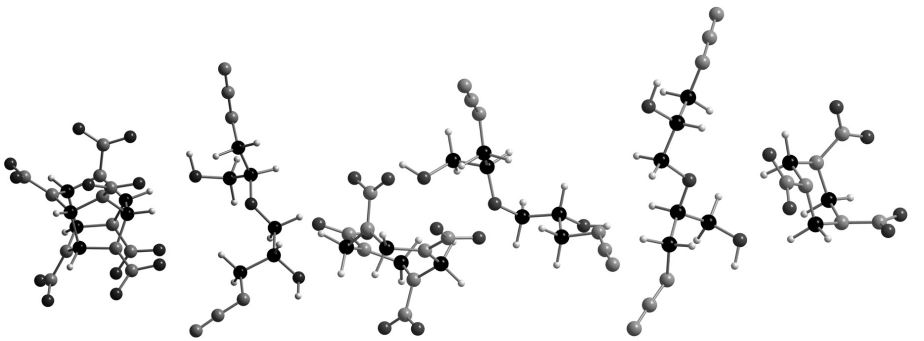

Figure 2. Alignment I of the mixtures of the nitramines HMX, RDX and CL20 with GAP.

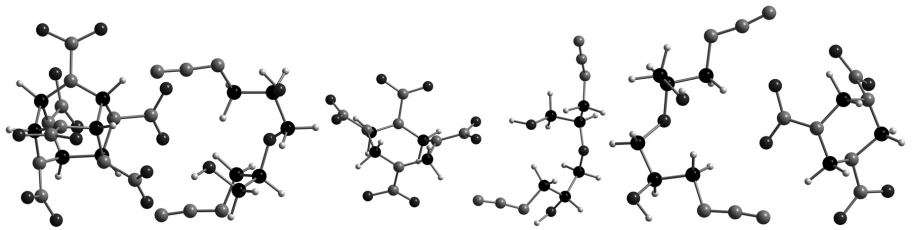

Figure 3. Alignment II of the mixtures of the nitramines HMX, RDX and CL20 with GAP.

NO_2 elimination

The homolytic N-NO_2 bond fission is the most important initial step of the decomposition of the nitramines [4, 8, 11, 13, 14, 16, 18, 21, 22, 25-27, 33]. Due to their different environments the NO_2 groups of each nitramine are not equivalent. As the decomposition is assumed to have no activation barrier, [13-15, 21, 22] a comparison of the product radicals of this decomposition step indicates the NO_2 groups which can be eliminated most easily (Table 2).

Table 2. Relative energies (kJ mol^{-1}) of the product radicals of the homolytic N-NO_2 bond fission (B3LYP/6-31G(d))

	HMX	RDX		CL20
axial	173.24	166.12	five membered ring (planar)	154.47
equatorial	164.46	168.28	five membered ring (non-planar)	148.77
			six membered ring	170.06

Table 3. Axial and equatorial elimination of HONO from HMX and RDX at the B3LYP/6-31G(d) level of theory

	axial elimination	equatorial elimination
HMX	204.42 (182.95)	203.64 (182.95)
RDX	184.84 (164.12)	194.56 (173.40)

The difference of 8.48 kJ mol^{-1} between the axial and equatorial HMX radicals is in agreement with the literature value of 12.13 kJ mol^{-1} [15]. In previous theoretical investigations of the elimination of NO_2 from RDX the triaxial conformation was used, in which all NO_2 groups are equivalent [21, 22]. The difference of 2.16 kJ mol^{-1} between the axial and equatorial elimination of NO_2 from diaxial RDX suggests only a very slight preference for the axial elimination. This would be difficult to determine experimentally as the equilibrium between different RDX conformations would also play a role. Low temperature EPR photolysis studies of CHO have shown that there is no preference for the elimination of a particular nitro group [30-32]. Our results show that the elimination of NO_2 from CL20 takes place in a five membered ring, the elimination of an NO_2 group coplanar to the ring system is favored by 4.70 kJ mol^{-1}. The elimination of NO_2 from CL20 is from a five membered ring is favored by 12.3 kJ mol^{-1} (13.8 kJ mol^{-1}) [33] over the elimination from a six membered ring.

The singlet and triplet reaction profile of the NO_2 elimination was determined by optimization of the singlet and triplet compounds at different N-NO_2 distances. The singlet-triplet crossover was found at 176.96 kJ mol^{-1} and an N-NO_2 distance of 2.381 Å for the equatorial N-NO_2 bond fission in HMX and at 173.02 kJ mol^{1} and an N-NO_2 distance of 2.428 Å for the axial N-NO_2 bond fission of RDX. The literature values at the same level of theory are about 10 kJ mol^{-1} lower in energy [15, 22]. Single point energy calculations only were performed for CL20 at different N-NO_2 distances due to the high computational cost.

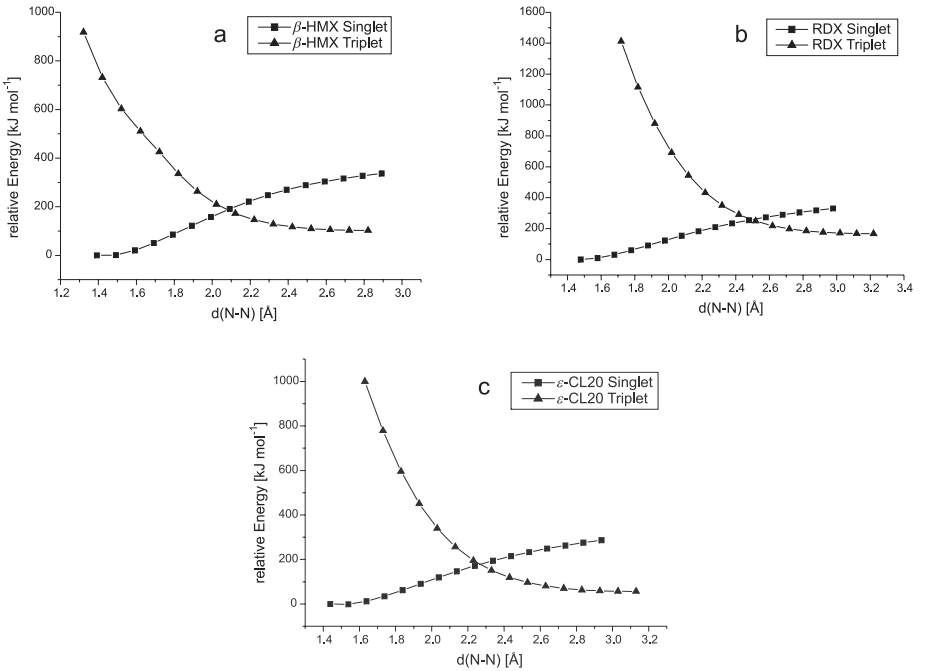

Figure 4. Reaction profile for the N-NO_2 bond fission of β-HMX (a), RDX (b) und ε-CL20 (c) at the B3LYP/3-21G level of theory.

The calculated bond fission energies agree with previously reported values (Table 1) [13-16, 21, 22]. As expected, the NO_2 elimination from CL20 is favored by 11.87 kJ mol^{-1} (9.70 kJ mol^{-1} with *zpe*) over the NO_2 elimination from HMX due to cage strain.

The comparison of the energies of the product radicals between the nitramines and their mixtures with GAP-diol shows only a small influence of the GAP-diol molecule on the decomposition reaction. The elimination of NO_2 from HMX is favored by 0.94 kJ mol^{-1} (1.59 kJ mol^{-1} with *zpe*) for alignment I; for alignment II the elimination step is 6.15 kJ mol^{-1} (6.52 kJ mol^{-1} with *zpe*) higher in energy. For CL20 the elimination of NO_2 from alignment I is favored by 3.07 kJ mol^{-1} (1.38 kJ mol^{-1} with *zpe*), and from alignment II by 8.01 kJ mol^{-1} (7.67 kJ mol^{-1} with *zpe*). In summary, the elimination of NO_2 from HMX and CL20 is more favorable in the presence of GAP, but more so for CL20 than for HMX. This is in agreement with the faster rate of decomposition of mixtures of CL20 with GAP-diol compared with mixtures of HMX with GAP [1]. For RDX

the bond dissociation energy is higher in the mixtures with GAP than for isolated RDX. Elimination from alignment I requires 24.50 kJ mol^{-1} (21.86 kJ mol^{-1} with *zpe*) higher in energy, and alignment II 2.65 kJ mol^{-1} (2.57 kJ mol^{-1} with *zpe*). For alignment II the product radical has a lower energy than in alignment I. This was also observed for CL20, while for HMX, alignment I is more favorable.

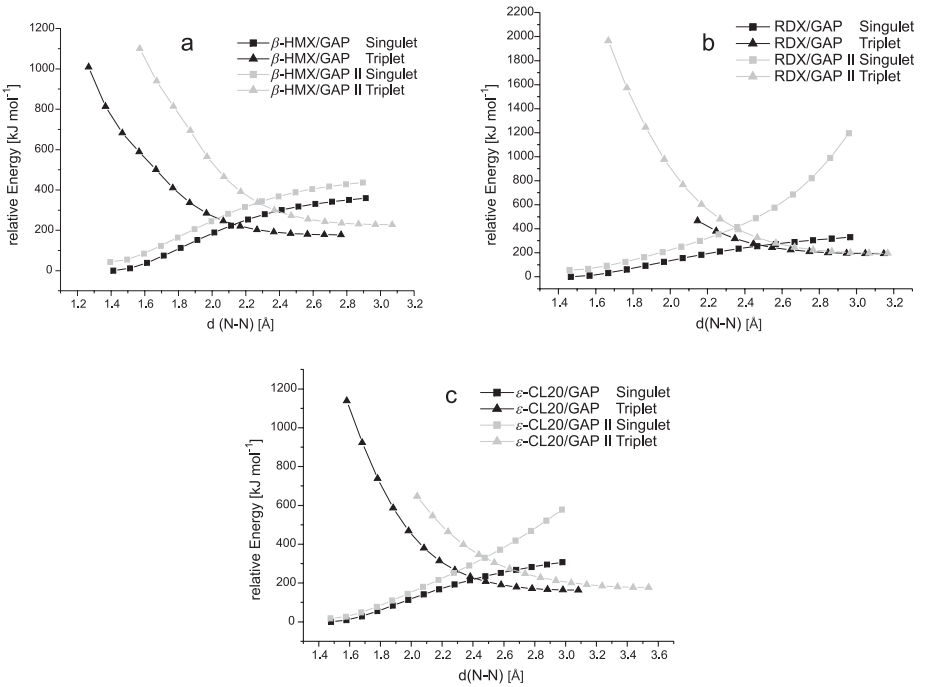

Figure 5. Reaction profile for the N-NO_2 bond fission of mixtures of β-HMX (a), RDX (b) and ε-CL20 (c) with GAP-diol at the B3LYP/3-21G level of theory.

We conclude that the presence of GAP-diol favors the N-NO_2 bond fission reaction of HMX and CL20 while it inhibits the N-NO_2 fission of RDX. The alignment of the molecules has a strong influence upon the extent to which the elimination of NO_2 is favored.

Conclusion

The reaction profiles for the N-NO_2 bond fission reaction in the mixtures of the nitramines HMX, RDX and CL20 with the energetic binder GAP (glycidyl azide polymer)-diol were investigated at the B3LYP/3-21G(d) level of theory and compared with the reaction profiles of the decomposition of the isolated nitramines and GAP-diol, which were calculated at the B3LYP level with 6-31G(d) and 3-21G basis sets. The following polymorphs were found as the minimum conformers: β-HMX, the diaxial conformation of RDX and β-CL20. For further calculations we used ε-CL20 because it is the commercially available material. The homolytic fission of an N-NO_2 bond is the most favorable initial decomposition step of the cyclic nitramines and even more so for CL20 due to its strained cage structure. The results obtained with the 3-21G basis set show the same tendencies as for the 6-31G(d) basis set.

The transition states of mixtures of the nitramines HMX, RDX and CL20 with GAP-diol were calculated for two different conformations, the minimum energy conformation and a conformation that was believed to be particularly favorable for the decomposition of the nitramines.

We found the activation energies for the two investigated conformations to be quite different and either conformation could favor or disfavor the homolytic N-NO_2 bond fission depending on the respective nitramine. For HMX the homolytic N-NO_2 bond fission in the mixture with GAP-diol is favored by 0.94 kJ mol^{-1} (1.59 kJ mol^{-1} with *zpe*) over isolated HMX, for CL20 it is favored by 8.01 kJ mol^{-1} (7.67 kJ mol^{-1} with *zpe*) and for RDX it is disfavored by 2.65 kJ mol^{-1} (2.57 kJ mol^{-1} with *zpe*)

Due to the great conformational flexibility of the system, the values given for the increases or decreases in energy over the isolated compounds for a given reaction pathway are only estimates and represent the upper limit for the actual activation energy of the system.

Computational Methods

All calculations were performed with the Gaussian 03 program at the B3LYP level using a 6-31G(d) and 3-21G basis sets [34]. The structures were minimized within the symmetry constraints stated above. All minima were confirmed by frequency analyses. The located transition states are of first order with Cartesian displacement coordinates of the imaginary frequency mode corresponding to a reaction of the starting materials to give the products.

Acknowledgement

We are grateful to the Leibniz Rechenzentrum for generous allocation of computer time. Kate Harris gratefully acknowledges financial support by the UK Socrates-Erasmus Council and TMK acknowledges financial support by the Fonds der Chemischen Industrie (FCI), the German WIWEB and the US Army Research Laboratory (ARL).

References

[1] Bohn M. A., Dörich M., Aniol J., Pontius H., Gerber P., Reactivity between ε-CL20-GAP and β-HMX-GAP Investigated by Mass Ioss, Adiabatic Self Heating and Dynamic Mechanical Analysis., *Proc. Int. Pyrotechnics Seminar* **2004**, *31st*, Fort Collins, Colorado, USA, 11.-16.07 2004.

[2] Bohn M. A., Thermal Ageing of Rocket Propellant Formulations Containing Epsilon-HNIW (epsilon-CL20) Investigated by Heat Generation Rate and Mass Loss., *Thermochim. Acta*, **2003**, *401*, 27-41.

[3] Bohn M. A., Kempa P. B., Thome V., Exploring of Interactions Between the Nitramines RDX, HMX, CL20 and Components in Formulations by Computer Simulation, *Int. Annu. Conf. ICT: Energetic Materials – Analysis, Diagnostics and Testing* **2000**, *31st*, 63/1-63/19; 27-30.6.2000.

[4] Bulusu S., Weinstein D. I., Autera J. R., Velicky R. W., Deuterium Kinetic Isotope Effect in theThermal Decomposition of 1,3,5-trinitro-1,3,5-triazacyclohexane and 1,3,5,7-tetranitro-1,3,5,7-tetraazacyclooctane: Its Use as an Experimental Probe for Their Shock-induced Chemistry., *J. Phys. Chem.*, **1986**, *90*, 4121-4126.

[5] Oxley J. C., Kooh A. B., Szekeres R., Zheng W., Mechanisms of Nitramine Thermolysis., *ibid.*, **1994**, *98*, 7004-7008.

[6] Palopoli S. F., Brill T. B., Thermal Decomposition of Energetic Materials. 52. On the Foam Zone and Surface Chemistry of Rapidly Decomposing HMX, *Combust. Flame*, **1991**, *87*, 45-60

[7] Shackelford S. A., Coolidge M. B., Goshgarian B. B., Loving B. A., Rogers R. N., Janney J. L., Ebinger M. H., Deuterium Isotope Effects in Condensed-phase Termochemical Decomposition Reactions of Octahydro-1,3,5,7-tetranitro-1,3,5,7-tetrazocine., *ibid.*, **1985**, *89*, 3118-3126.

[8] Brill T. B., Karpowicz R. J., Solid Phase Transition Kinetics. The Role of Intermolecular Forces in the Condensed-phase Decomposition of Octahydro-1,3,5,7-tetranitro-1,3,5,7-tetrazocine., *ibid.*, **1982**, 86, 4260-4265.

[9] Behrens R. Jr., Identification of Octahydro-1,3,5,7-tetranitro-1,3,5,7-tetrazocine (HMX) Pyrolysis Products by Simultaneous Thermogravimetric Modulated-beam Mass Spectrometry and Time-of-flight Felocity-spectra Measurements., *Int. J. Chem. Kinet.*, **1990**, *22*, 135-157.

[10] Behrens R. Jr., Determination of the Rates of Formation of Gaseous Products from the Pyrolysis of Octahydro-1,3,5,7-tetranitro-1,3,5,7-tetrazocine (HMX) by Simultaneous Thermogravimetric Modulated-beam Mass Spectrometry., *Int. J. Chem. Kinet.*, **1990**, *22*, 159-173.

[11] Behrens Jr. R., Thermal Decomposition of Energetic Materials: Temporal Behaviors of the Rates of Formation of the Gaseous Pyrolysis Products from Condensed-phase Decomposition of Octahydro-1,3,5,7-tetranitro-1,3,5,7-tetrazocine., *J. Phys. Chem.*, **1990**, *94*, 6708-6718.

[12] Behrens Jr. R., Bulusu S., Thermal Decomposition of Energetic Materials. 2. Deuterium Isotope Effects and Isotopic Scrambling in Condensed-phase Decomposition of Octahydro-1,3,5,7-tetranitro-1,3,5,7-tetrazocine., *ibid.*, **1991**, *95*, 5838-5845.

[13] Zhang S., Nguyen H. N., Truong T. N., Theoretical Study of Mechanisms, Thermodynamics, and Kinetics of the Decomposition of Gas-Phase α-HMX (Octahydro-1,3,5,7-tetranitro-1,3,5,7-tetrazocine)., *J. Phys. Chem. A*, **2003**, *107*, 2981-2989.

[14] Lewis J. P., Glaesemann K. R., VanOpdorp K., Voth G. A., *Ab Initio* Calculations of Reactive Pathways for a-Octahydro-1,3,5,7-tetranitro-1,3,5,7-tetrazocine (α-HMX)., *ibid.*, **2000**, *104*, 11384-11389.

[15] Chakraborty D., Muller R. P., Dasgupta S. and. Goddard III W. A, Mechanism for Unimolecular Decomposition of HMX (1,3,5,7-Tetranitro-1,3,5,7-tetrazocine), an *ab Initio* Study., *ibid.*, **2001**, *105*, 1302-1314.

[16] Shaw R., Walker F. E., Estimated Kinetics and Thermochemistry of Some Initial Unimolecular Reactions in the Thermal Decomposition of 1,3,5,7-tetranitro-1,3,5,7-tetraazacyclooctane in the Gas Phase., *J. Phys. Chem.*, **1977**, *81*, 2572-2576.

[17] Behrens R., Jr., Bulusu S., Thermal Decomposition of Energetic Materials. 3. Temporal Behaviors of the Rates of Formation of the GaseousPyrolysis Products from Condensed-phase Decomposition of 1,3,5-trinitrohexahydro-s-triazine (RDX)., *ibid.*, **1992**, *96*, 8877-8891.

[18] Wight C. A., Botcher T. R., Thermal Decomposition of Solid RDX Begins with Mitrogen-nitrogen Bond Scission., *J. Am. Chem. Soc.*, **1992**, *114*, 8303-8304.

[19] Behrens R., Jr., Bulusu S., Thermal Decomposition of Energetic Materials. 4. Deuterium Isotope Effects and Isotopic Scrambling (H/D, 13C/18O, 14N/15N) in Condensed-phase Decomposition of 1,3,5-trinitrohexahydro-s-triazine (RDX)., *J. Phys. Chem.*, **1992**, *96*, 8891-8897.

[20] Zhao X., Hintsa E. J., Lee Y. T., Infrared Multiphoton Dissociation of RDX (hexahydro-1,3,5-trinitro-1,3,5-triazine) in a Molecular Beam., *ibid.*, **1988**, *88* , 801-810.

[21] Wu C. J., Fried L. E., *Ab Initio* Study of RDX Decomposition Mechanisms., *ibid.*, **1997**, *101*, 8675-8679.

[22] Chakraborty D., Muller R. P., Dasgupta S., Goddard III W. A., The Mechanism for Unimolecular Decomposition of RDX (1,3,5-Trinitro-1,3,5-triazine), an *ab Initio* Study., *J. Phys. Chem. A*, **2000**, *104*, 2261-2272.

[23] Harris N. J., Lammertsma K., *Ab Initio* Density Functional Computations of Conformations and Bond Dissociation Energies for Hexahydro-1,3,5-trinitro-1,3,5-triazine., *J. Am. Chem. Soc.*, **1997**, *119*, 6583-6589.

[24] Nedelko V. V., Chukanov N. V., Raevskii A. V., Korsounskii B. L., Larikova T. S., Kolesova O. I., Volk F., Comparative Investigation of Thermal Decomposition of Various Modifications of Hexanitrohexaazaisowurtzitane (CL-20)., *Propell. Explos. Pyrotech.*, **2000**, *25*, 255-259.

[25] Patil D. G., Brill T. B., Thermal Decomposition of Energetic Materials. 53. Kinetics and Mechanism of Thermolysis of Hexanitrohexazaisowurtzitane., *Combust. Flame*, **1991**, *87*, 145-151.

[26] Löbbecke S., *PhD. Thesis*, Philipps-Universität Marburg **1999**.

[27] Löbbecke S., Bohn M. A., Pfeil A., Krause H., Thermal Behavior and Stability of HNIW (CL20), *29th Int. Annual Conf. of ICT*, Karlsruhe **1998**.

[28] M. A. Bohn, Kinetic Description of Mass Loss Data for theAssessment of Stability, Compatibility and Aging of Energetic Components and Formulations Exemplified with ε-CL20., *Propell. Explos. Pyrotech.*, **2002**, *27*, 125-135.

[29] Patil D. G., Brill T. B., Thermal Decomposition of Energetic Materials. 59. Characterization of the Residue of Hexanitrohexaazaisowurtzitane., *Combust. Flame*, **1993**, *92*, 456-458.

[30] Ryzhkov L. R., McBride J. M., Low-Temperature Reactions in Single Crystals of Two Polymorphs of the Polycyclic Nitramine 15N-HNIW. *J. Phys. Chem.*, **1996**, *100*, 163-169.

[31] Ryzhkov L. R., McBride J. M., Structure, Motion, and Exchange Coupling of $15NO_2$/ /$15NO_2$ Radical Pairs Occupying Adjacent Solvent Cavities of α-HNIW, a Nitramine Hydrate., *J. Am. Chem. Soc.*, **1997**, *119*, 4826-4833.

[32] Pace M. D., EPR Spectra of Photochemical Nitrogen Dioxide Formation in Monocyclic Nitramines and Hexanitrohexaazaisowurtzitane., *J. Phys. Chem.*, **1991**, *95*, 5858-5864.

[33] Okovytyy S., Kholod Y., Qasim M., Fredrickson H., Leszynski J., The Mechanism of Unimolecular Decomposition of 2,4,6,8,10,12-Hexanitro-2,4,6,8,10,12-hexaazaisowurtzitane. A Computational DFT Study, *J. Phys. Chem. A*, **2005**, *109*, 2964-2970.

[34] Frisch M. J., Trucks G. W., Schlegel H. B., Scuseria G. E., Robb M. A., Cheeseman J. R., Zakrzewski V. G., J. A. M. Jr., Stratmann R. E., Burant J. C., Dapprich S., Millam J. M., Daniels A. D., Kudin M. C. S. K. N., Farkas O., Tomasi J., Barone V., Cossi M., Cammi R., Mennucci B., Pomelli C., Adamo C., Clifford S., Ochterski J., Petersson G. A., Ayala P. Y., Cui Q., Morokuma K., Malick D. K., Rabuck A. D., Raghavachari K., Foresman J. B., Cioslowski J., Ortiz J. V., Baboul A. G., Stefanov B. B., Liashenko A., Liu G., Piskorz P., Komaromi I., Gomperts R., Martin R. L., Fox D. J., Keith T., Al-Laham M. A., Peng C. Y., Nanayakkara A., Gonzalez C., Challacombe M., Gill P. M. W., Johnson B., Chen W., Wong M. W., Andres J. L., Gonzalez C., Head-Gordon M., Replogle E. S., Pople J. A., Gaussian98, Revision A.8, Pittsburgh PA **1998**.